molecules

MDPI

Article

New Triterpenoids and Anti-Inflammatory Constituents from *Glinus oppositifolius*

Jih-Jung Chen [1,2,†], Chang-Syun Yang [1,†], Yu-Hui Chen [3], Che-Yi Chao [4], Yu-Chang Chen [5] and Yeuh-Hsiung Kuo [3,6,7,*]

1 Department of Pharmacy, School of Pharmaceutical Sciences, National Yang Ming Chiao Tung University, Taipei 112304, Taiwan; jjungchen@nycu.edu.tw (J.-J.C.); tim0619@nycu.edu.tw (C.-S.Y.)
2 Department of Medical Research, China Medical University Hospital, China Medical University, Taichung 404327, Taiwan
3 Department of Chinese Pharmaceutical Sciences and Chinese Medicine Resources, China Medical University, Taichung 404327, Taiwan; chenyh2@airproducts.com
4 Department of Food Nutrition and Health Biotechnology, Asia University, Taichung 41354, Taiwan; chenyj@asia.edu.tw
5 School of Pharmacy, College of Pharmacy, Kaohsiung Medical University, Kaohsiung 807377, Taiwan; yuchang@kmu.edu.tw
6 Chinese Medicine Research Center, China Medical University, Taichung 404327, Taiwan
7 Department of Biotechnology, Asia University, Taichung 413305, Taiwan
* Correspondence: kuoyh@mail.cmu.edu.tw; Tel.: +886-4-2205-3366-5701
† These authors contributed equally to this work.

Abstract: Three new triterpenoids—spergulagenin B (**1**), spergulagenin C (**2**), and spergulagenin D (**3**)—were isolated from the aerial part of *Glinus oppositifolius*, along with 17 known compounds (**4**–**20**). The structures of these new compounds were identified by spectroscopic and MS analyses. Compounds **3**, **5**, **19**, and **20** were evaluated for inhibition of nitric oxide production in LPS-stimulated RAW 264.7 cells with IC_{50} values of 17.03, 18.21, 16.30, and 12.64 μM, respectively. Compounds **3**, **5**, and **20** exhibited inhibitory effects on LPS-induced nitric oxide production in RAW 264.7 cells with IC_{50} values of 18.35 ± 1.34, 17.56 ± 1.41, and 14.27 ± 1.29 μM, respectively.

Keywords: Molluginaceae; *Glinus oppositifolius*; triterpenoids; spergulagenin A; spergulagenin B; spergulagenin C; anti-inflammatory activity

Citation: Chen, J.-J.; Yang, C.-S.; Chen, Y.-H.; Chao, C.-Y.; Chen, Y.-C.; Kuo, Y.-H. New Triterpenoids and Anti-Inflammatory Constituents from *Glinus oppositifolius*. *Molecules* **2023**, *28*, 2903. https://doi.org/10.3390/molecules28072903

Academic Editor: Raluca Maria Pop

Received: 21 February 2023
Revised: 20 March 2023
Accepted: 21 March 2023
Published: 23 March 2023

1. Introduction

Molluginaceae has about 13 genera and more than 120 kinds of plants in the world, mainly distributed in tropical and subtropical regions. *Glinus oppositifolius* (L.) Aug. DC. (Figure 1) is an annual herb mainly distributed at low altitudes in the southern part of Taiwan [1]. *G. oppositifolius* is a folk herb used in the treatment of dermatitis and chronic inflammatory diseases [2]. Flavonoids [3,4], triterpenoids [4], naphthalenes [4], and their derivatives are widely distributed in plants of the family Molluginaceae. Many of these compounds exhibit anti-inflammatory [3,5], antifungal, antiparasitic, and antibacterial activities [6]. Macrophages are one of the immune cells that can secrete nitric oxide (NO), a mediator of inflammatory responses that can participate in host defense [7]. Tumor necrosis factor alpha (TNF-α) is a cytokine with pleiotropic effects on a variety of cell types. It has been recognized as a master regulator of inflammatory responses and has a bearing on the pathogenesis of certain inflammatory diseases [8]. Inhibition of abnormal activation of macrophages by medicines has been proposed as a way to improve inflammatory diseases. *G. oppositifolius* was one of many species that we screened for the anti-inflammatory constituents of Formosan plants. Current phytochemical studies of *G. oppositifoliu* have led to the isolation of three new triterpenoids—spergulagenin B (**1**), spergulagenin C (**2**),

and spergulagenin D (**3**)—together with 17 known compounds. This article describes the structural elucidation of **1**–**3** and the anti-inflammatory activity of the isolated compounds.

Figure 1. Plant material: *Glinus oppositifolius* (L.) Aug. DC.

2. Materials and Methods

2.1. General

Infrared (IR) spectra (KBr or neat) were measured using a Shimadzu IR prestige-21 Fourier transform infrared spectrophotometer (Shimadzu, Kyoto, Japan). Optical rotations were recorded on a Jasco P-1020 polarimeter (Jasco, Kyoto, Japan) in MeOH and $CHCl_3$. Electronic circular dichroism (ECD) spectra were recorded on a Chirascan CD spectrometer (Applied Photophysics Ltd., Leatherhead, UK). High resolution electron ionization mass spectrometry (HR-EI-MS) was measured at Chung Hsing University (Taichung, Taiwan). Ultraviolet (UV) spectra were measured using a Shimadzu Pharmaspec-1700 UV-Visible spectrophotometer (Shimadzu, Kyoto, Japan). Nuclear magnetic resonance (NMR) spectra—including heteronuclear single-quantum coherence (HSQC), correlation spectroscopy (COSY), heteronuclear multiple-bond correlation (HMBC), and nuclear Overhauser effect spectrometry (NOESY) experiments—were measured using a Bruker DRX-500 FT-NMR (Bruker, Bremen, Germany) operating at 125 MHz (^{13}C) and 500 MHz (^{1}H), respectively. Chemical shifts are given in ppm (δ) using tetramethylsilane (TMS) as internal standard. HPLC separations were carried out utilizing a P230 HPLC system (NATIONAL ANALYTICAL CORPORATION, Maharashtra, India) equipped with P230 HPLC Pump and an IOTA 2 detector, utilizing ChromNav software (version 2.0, Jasco). TLC analysis was performed utilizing aluminum pre-coated Si plates (Merck, Darmstadt, Germany). Column chromatography was carried out utilizing LiChroCART Si gel (5 μM) (Merck, Darmstadt, Germany).

2.2. Chemicals

ACS grade solvents (methanol, ethyl acetate, *n*-hexane, acetone, and chloroform), HPLC grade solvents (ethyl acetate, acetone, and *n*-hexane) and deuterated solvents ($CDCl_3$, acetone-d_6, or CD_3OD) for NMR measurements were procured from Merck, Taipei, Taiwan. LPS (endotoxin from *Escherichia coli*, serotype 0127:B8), Carr (type IV), and quercetin were purchased from MedChemExpress (Monmouth Junction, NJ, USA). MTT (3-[4,5-dimethylthiazol-2-yl]-2,5-diphenyltetrazolium bromide) was acquired from Sigma Chemical Co. (St. Louis, MO, USA).

2.3. Plant Material

Glinus oppositifolius was collected from Neipu Township, Pingtung County, Taiwan, in February 2010 and identified by J.-J. Chen. A voucher specimen (GO-100514) was deposited in the Department of Pharmacy, National Yang Ming Chiao Tung University, Taipei, Taiwan.

2.4. Extraction and Isolation

The dried whole plant (10.58 kg) of *Glinus oppositifolius* was extracted 3 times with methanol (80 L each) for 7 days. The extract was concentrated under reduced pressure at 38 °C, and the residue (1.48 kg) was partitioned between H_2O and EtOAc (1:1) to provide the EtOAc-soluble fraction (fraction A, 285 g). Fraction A (285 g) was separated by column chromatography (CC) (10.0 kg of SiO_2, 70–230 mesh; *n*-hexane/EtOAc/methanol gradient) to afford 20 fractions: A1–A20.

Fraction A13 (7.69 g) was purified by Sephadex LH 20 CC (chloroform:methanol = 3:7), silica gel CC (*n*-hexane:acetone = 8:3), and then HPLC (chloroform:acetone = 6:1) to obtain **4** (12.8 mg), **5** (27.4 mg), **6** (12.2 mg), **7** (8.4 mg), and **5** (7.3 mg). Fraction A14 (16.7 g) was purified by silica gel CC (ethyl acetate: *n*-hexane = 1:6) and HPLC (acetone:*n*-hexane = 1:8) to obtain **6** (12.6 mg), **7** (6.4 mg), and **8** (13.4 mg). Fraction A16 (15.5 g) was purified by silica gel CC (*n*-hexane:ethyl acetate = 4:1) and HPLC (*n*-hexane:acetone = 3:1) to obtain **9** (8.2 mg), **10** (27.5 mg), **11** (25.0 mg), **12** (8.4 mg), **13** (13.4 mg), **14** (24.5 mg), **15** (7.8 mg), **16** (6.2 mg), **17** (4.3 mg), **18** (32.4 mg), **19** (4.5 mg), and **20** (32.4 mg). Fraction A18 (13.3 g) was purified by Sephadex LH 20 CC (chloroform:methanol = 3:7), silica gel CC (*n*-hexane:acetone = 5:1), and then semi-preparative HPLC (chloroform: ethyl acetate = 3:2) to obtain **1** (6.6 mg), **2** (4.2 mg), and **3** (3.6 mg).

Spergulagenin B (**1**): colorless needle; mp 306.2–307.6 °C; IR (KBr) υ_{max}: 3423 (OH), 2943, 1694 (C=O), 1458, 1385, 1155, 1113, 1061 cm^{-1} (Figure S1); ^{1}H-NMR spectroscopic data, see Table 1 (Figure S2); ^{13}C-NMR spectroscopic data, see Table 2 (Figure S3); ECD (*c* 0.25, MeOH) λ_{ma} ($\Delta\varepsilon$) 284 (+0.88), 250 (–0.12), 217 (+0.98), 198 (–1.34) nm; HI-EI-MS: 472.3549 $[M]^+$ (calcd. for $C_{30}H_{48}O_4$, 472.3547).

Table 1. ^{1}H-NMR data for Compounds **1**–**3** (δ in ppm, *J* in Hz).

Position	1 [a]	2 [a]	3 [a]
1	1.94 (m). 1.41 (m)	7.10 (d, *J* = 10.0 Hz)	1.82 (m), 1.39 (m)
2	2.48 (m), 2.42 (m)	5.83 (d, *J* = 10.0 Hz)	2.52 (m), 2.38 (ddd, *J* = 16.0, 5.6, 3.2 Hz)
5	1.30 (m)	1.54 (m)	1.33 (m)
6	1.51 (m), 1.37 (m)	1.56 (m), 1.43 (m)	1.60 (m), 1.35 (m)
7	1.50 (m), 1.31 (m)	1.50 (m), 1.44 (m)	1.54 (m), 1.47 (m)
9	1.69 (m)	1.59 (m)	1.70 (dd, *J* = 9.6, 4.4Hz)
11	1.87 (m), 1.04 (m)	1.57 (m), 1.46 (m)	2.25 (m), 2.22 (m)
12	3.96	3.99 (m)	
13	1.38 (d, *J* = 4.0 Hz)	1.43 (m)	2.23 (m)
15	1.72 (dd, *J* = 12.8, 4.0 Hz), 1.35 (m)	1.72 (m), 1.32 (m)	1.79 (m), 1.44 (m)
16	3.70 (m)	3.71 (m)	3.76 (m)
17	1.76 (d, *J* = 11.2 Hz)	1.78 (m)	1.64 (m)
19	2.02 (m), 1.27 (m)	2.04 (m), 1.28 (m)	2.17 (m), 1.02 (m)
20	2.05 (m), 1.84 (m)	2.05 (m), 1.86 (m)	2.10 (m), 1.93 (m)
23	1.03 (s)	1.09 (s)	1.06 (s)
24	1.08 (s)	1.14 (s)	1.10 (s)
25	0.96 (s)	1.08 (s)	1.00 (s)
26	1.07 (s)	1.11 (s)	1.21 (s)
27	1.01 (s)	1.01 (s)	0.99 (s)
28	1.04 (s)	1.05 (s)	1.14 (2)
29	1.43 (s)	1.45 (s)	1.43 (s)
30	2.23 (s)	2.24 (s)	2.24 (s)

[a] measured in $CDCl_3$ at 500 MHz.

Table 2. ^{13}C-NMR data for Compounds **1**–**3** (δ in ppm).

Position	1 [a]	2 [a]	3 [a]
1	39.4	158.5	38.9
2	34.0	125.6	34.1
3	217.3	205.3	216.9
4	48.1	39.2	47.6
5	54.9	53.3	55.1
6	19.7	19.1	19.9
7	32.5	32.6	32.0
8	45.5	45.5	47.2
9	47.3	42.7	49.6
10	36.7	44.6	37.0
11	32.9	32.5	39.6
12	69.5	69.3	210.9
13	55.1	55.2	63.4
14	41.4	42.3	41.6
15	45.1	45.0	43.8
16	65.8	65.7	65.8
17	59.2	59.2	58.7
18	46.3	46.3	44.9
19	44.1	44.0	41.7
20	35.9	35.8	35.8
21	54.4	54.4	55.6
22	217.2	217.0	217.3
23	21.1	21.4	21.4
24	26.6	27.8	26.6
25	15.6	17.1	15.2
26	16.6	17.2	16.7
27	18.7	18.9	20.9
28	17.2	18.8	17.7
29	21.2	21.1	21.4
30	25.9	25.9	26.1

[a] measured in $CDCl_3$ at 125 MHz.

Spergulagenin C (**2**): colorless needle; mp 305.4–306.8 °C; UV (MeOH) λ_{max} nm (log λ): 229 (3.73); IR (KBr) υ_{max}: 3493 (OH), 3416 (OH), 2972, 1690 (C=O), 1458, 1385, 1355, 1254, 1076 cm^{-1} (Figure S9); ^{1}H-NMR spectroscopic data, see Table 1 (Figure S10); ^{13}C-NMR spectroscopic data, see Table 2 (Figure S11); ECD (*c* 0.18, MeOH) λ_{max} (Δε) 283 (+0.96), 249 (–0.14), 219 (+1.05), 198 (–1.09) nm; HI-EI-MS: 470.3409 [M]$^{+}$ (calcd. for $C_{30}H_{46}O_4$, 470.3406).

Spergulagenin D (**3**): colorless needle; mp 286.4–287.0 °C; IR (KBr) υ_{max}: 3447 (OH), 2938, 1697 (C=O), 1558, 1420, 1387, 1354, 1327 cm^{-1} (Figure S17); ^{1}H-NMR spectroscopic data, see Table 1 (Figure S18); ^{13}C-NMR spectroscopic data, see Table 2 (Figure S19); ECD (*c* 0.21, MeOH) λ_{max} (Δε) 284 (+1.02), 249 (–0.20), 218 (+1.02), 197 (–0.91) nm; HI-EI-MS: 470.3407 [M]$^{+}$ (calcd. for $C_{30}H_{46}O_4$, 472.3403).

Kaempferol (**4**): yellow powder; mp 274~276 °C; IR (KBr) υ_{max}: 3348, 3278~2509, 1661, 1616, 1570, 1089, 1010 cm^{-1}; ^{1}H -NMR (500 MHz, acetone-d$_6$) δ (ppm): 6.26 (1H, d, *J* = 1.9 Hz, H-6), 6.52 (1H, d, *J* = 1.9 Hz, H-8), 7.01 (2H, d, *J* = 8.9 Hz, H-3′ and H-5′), 8.14 (2H, d, *J* = 8.9 Hz, H-2′ and H-6′), 12.15 (1H, s, OH-5).

6,8-Dimethyl-5,7,4′-trihydroxyflavone (**5**): yellow powder; mp 220~225 °C; IR (KBr) υ_{max}: 3427, 3704~2509, 1654, 1611, 1576, 1555 cm^{-1}; ^{1}H-NMR (500 MHz, acetone-d$_6$) δ (ppm): 2.13 (3H, s, Me-6), 2.36 (3H, s, Me-8), 6.64 (1H, s, H-3), 7.05 (2H, d, *J* = 8.8 Hz, H-3′, H-5′), 7.98 (2H, d, *J* = 8.8 Hz, H-2′ and H -6′), 13.24 (1H, s, OH-5).

5,7-Dihydroxy-6,8-dimethylflavone (**6**): yellow powder; mp 289~290 °C; IR (KBr) υ_{max}: 3400, 3587~2403, 1650, 1602, 1486 cm^{-1}; ^{1}H-NMR (500 MHz, acetone-d$_6$) δ (ppm): 2.19 (3H, s, Me-6), 2.37 (3H, s, Me-8), 6.68 (1H, s, H-3), 7.54 (3H, m, H-3′, H-4′ and H-5′), 7.91 (2H, d, *J* = 7.2 Hz, H-2′ and H-6′), 12.95 (1H, s, OH-5).

5,4′-Dihydroxy-7-methoxy-6,8-dimethylflavone (**7**): yellow powder; mp 286~287 °C; IR (KBr) υ_{max}: 3502~2423, 3430, 3072, 2920, 1650, 1612, 1585, 1466 cm^{-1}; ^{1}H-NMR (500 MHz, $CDCl_3$) δ (ppm): 2.18 (3H, s, Me-6), 2.36 (3H, s, Me-8), 3.90 (3H, s, OMe-7), 5.40 (1H, s, OH -4′), 6.89 (1 H, s, H-3), 7.03 (2H, d, *J* = 8.8 Hz, H-3′ and H-5′), 7.87 (2H, d, *J* = 8.8 Hz, H-2′ and H-6′), 13.03 (1H, s, OH-5).

4-Hydroxybenzoic acid (**8**): white solid; mp 210~212 °C; IR (KBr) υ_{max}: 3300~2500, 1696 cm^{-1}; ^{1}H-NMR (500 MHz, $CDCl_3$) δ (ppm): 6.33 (1H, br s, Ar-OH), 6.81 (2H, d, *J* = 8.8 Hz, H-3 and H -5), 7.87 (2H, d, *J* = 8.8 Hz, H-2 and H-6).

4-Hydroxybenzaldehyde (**9**): white solid; mp 110~112 °C; IR (KBr) υ_{max}: 3170, 1676, 1600, 1519, 1454 cm^{-1}; ^{1}H-NMR (500 MHz, $CDCl_3$) δ (ppm): 5.81 (1H, s, Ar-OH), 6.95 (2H, d, *J* = 8.4 Hz, H-3 and H-5), 7.81 (2H, d, *J* = 8.4 Hz, H-2 and H-6), 9.87 (1H, s, CHO).

4-Hydroxyacetophenone (**10**): white solid; mp 106~107 °C; IR (KBr) υ_{max}: 3312, 1664, 1602, 1578 cm^{-1}; ^{1}H-NMR (500 MHz, $CDCl_3$) δ (ppm): 2.56 (3H, s, COMe), 6.09 (1H, s, Ar-OH), 6.89 (2H, d, *J* = 8.8 Hz, H-3 and H-5), 7.91 (2H, d, *J* = 8.8 Hz, H-2 and H-6).

Methyl 4-Hydroxybenzoate (**11**): white solid; mp 124~125 °C; IR (KBr) υ_{max}: 3358, 1689, 1608, 1585, 1514 cm^{-1}; ^{1}H-NMR (500 MHz, $CDCl_3$) δ (ppm): 3.89 (3H, s, COOMe), 5.37 (1H, s, Ar-OH), 6.95 (2H, d, *J* = 8.0 Hz, H-3 and H -5), 7.95 (2H, d, *J* = 8.0 Hz, H-2 and H-6).

p-Anisic acid (**12**): white solid; mp 182~184°C; IR (KBr) υ_{max}: 3307~2503, 2926, 1686, 1605, 1578, 1516 cm^{-1}; ^{1}H-NMR (500 MHz, $CDCl_3$) δ (ppm): 3.85 (3H, s, OMe-4), 6.97 (2H, d, *J* = 8.8 Hz, H-3 and H-5), 7.96 (2H, d, *J* = 8.8 Hz, H-2 and H-6).

Vanillin (**13**): white solid; mp 210~212 °C; IR (KBr) υ_{max}: 3213, 2724, 2858, 1667, 1589, 1510 cm^{-1}; ^{1}H-NMR (500 MHz, $CDCl_3$) δ (ppm): 3.97 (3H, s, OMe-3), 6.21 (1H, s, Ar-OH), 7.04 (1H, d, *J* = 8.0 Hz, H-5), 7.42 (1H, d, *J* = 2.0 Hz, H-2), 7.43 (1H, dd, *J* = 8.0, 2.0 and H-6), 9.83 (1H, s, CHO).

4-Hydroxy-3-methoxyacetophenone (**14**): white solid; mp 182~184 °C; IR (KBr) υ_{max}: 3323, 2912, 1658, 1575, 1518 cm^{-1}; ^{1}H-NMR (500 MHz, $CDCl_3$) δ (ppm): 2.56 (3H, s, COMe), 3.96 (3H, s, OMe-3), 6.05 (1H, s, Ar-OH), 6.95 (1H, d, *J* = 8.0 Hz), 7.54 (2H, br s, H-2 and H-6).

Acetosyringone (**15**): white solid; mp 105~107 °C; IR (KBr) υ_{max}: 3307, 1672, 1608 cm^{-1}; ^{1}H-NMR (500 MHz, $CDCl_3$) δ (ppm): 2.57 (3H, s, COMe), 3.96 (6H, s, OMe-3, OMe-5), 6.05 (1H, s, Ar-OH), 7.25 (2H, s, H-2 and H-6).

4-Hydroxy-3, 5-dimethoxybenzaldehyde (**16**): white solid; mp 112~114 °C; IR (KBr) υ_{max}: 3410, 2727, 1685, 1605, 1514 cm^{-1}; ^{1}H -NMR (500 MHz, $CDCl_3$) δ (ppm): 3.98 (6H, s, OMe-3, OMe-5), 5.91 (1H, s, Ar-OH), 7.15 (2H, s, H-2 and H-6), 9.82 (1H, s, CHO).

4-Hydroxybenzyl alcohol (**17**): white solid; mp 116–117 °C; IR (KBr) υ_{max}: 3370, 1585, 1512 cm^{-1}; ^{1}H-NMR (500 MHz, $CDCl_3$) δ (ppm): 4.62 (2H, s, H-7), 4.79 (1H, s, Ar-OH), 6.82 (2H, d, *J* = 8.4 Hz, H-3 and H-5), 7.25 (2H, d, *J* = 8.4 Hz, H-2 and H-6).

2-(4-Hydroxyphenyl)ethanol (**18**): white solid; mp 92~93 °C; IR (KBr) υ_{max}: 3392, 1599, 1514 cm^{-1}; ^{1}H-NMR (500 MHz, $CDCl_3$) δ (ppm): 2.80 (2H, t, *J* = 8.0 Hz, H-7), 3.83 (2H, br. t, *J* = 8.0 Hz, H-8), 4.75 (1H, s, Ar-OH), 6.79 (2H, d, *J* = 8.0 Hz, H-3 and H-5), 7.10 (2H, d, *J* = 8.0 Hz, H-2 and H-6).

Cinnamic acid (**19**): white solid; mp 133~135 °C; IR (KBr) υ_{max}: 3267~2582, 2962, 1684, 1629 cm^{-1}; ^{1}H-NMR (500 MHz, $CDCl_3$) δ (ppm): 6.49 (1H, d, *J* = 16.0 Hz, H-8), 7.41 (3H, m, H-3, H-4 and H-5), 7.60 (2H, dd, *J* = 7.6, 2.0 Hz, H-2 and H-6), 7.68 (1H, d, *J* = 16.0 Hz, H-7).

trans-Ferulic acid (**20**): white solid, mp 168~169 °C; IR (KBr) υ_{max}: 3435, 3481~2750, 1690, 1662, 1515 cm^{-1}; ^{1}H-NMR (500 MHz, acetone-d_6) δ (ppm): 3.89 (3H, s, OMe-3), 6.30 (1H, d, *J* = 15.0 Hz, H-8), 6.80 (1H, d, *J* = 8.0 Hz, H-5), 7.05 (1H, d, *J* = 8.0 Hz, H-6), 7.17 (1H, s, H-2), 7.59 (1H, d, *J* = 15.0 Hz, H-7), 8.17 (1H, br s, Ar-OH).

2.5. Cell Culture

Murine RAW264.7 macrophages were cultured in DMEM medium containing 10% fetal bovine serum (FBS) and 1% penicillin at 37 °C, 5% CO_2 [9].

2.6. MTT assay

The MTT assay was performed by the reference method with slight modifications [9].

2.7. Nitric Oxide Inhibitory Assay

The NO inhibition assay was followed with a slight modification of the reference method [10].

2.8. Enzyme-Linked Immunosorbent Assay

RAW264.7 cells (4×10^5 cells in 96 well plates) were pre-treated with isolated compounds or vehicle (0.05% DMSO) for 1 h and then stimulated with LPS (100 ng/mL) for 20 h. Supernatants were collected and analyzed for production of TNF-α by using appropriate ELISA kits (R&D, Minneapolis, MN, USA) in accordance to the manufacturer's instructions.

2.9. Statistical Analysis

All the data are expressed as mean ± SEM. Statistical analysis was carried out using the Student's *t*-test. A probability of 0.05 or less was considered statistically significant. All the experiments were performed at least 3 times.

3. Results and Discussion

3.1. Isolation and Structural Elucidation

Chromatographic isolation of the EtOAc-soluble fraction of MeOH extract of aerial part of *G. oppositifolius* on column chromatography and high-performance liquid chromatography (HPLC) afforded three new triterpenoids—spergulagenin B (**1**), spergulagenin C (**2**), and spergulagenin D (**3**)—and 17 known compounds **4**–**20** (Figure 2).

Spergulagenin B (**1**) was isolated as colorless needle with molecular formula $C_{30}H_{48}O_4$ as confirmed by HR-EI-MS, showing an $[M]^+$ ion at *m/z* 472.3549 (calcd. 472.3547) and supported by the ^{1}H- and ^{13}C-NMR data. The IR absorption bands implied the presence of OH (3423 cm^{-1}) and acetyl group (1694 cm^{-1}). The ^{1}H- and ^{13}C-NMR data of **1** showed the acetyl group [δ_H 2.23 (3H, s, H-30); δ_C 25.9 (C-30) and 217.2 (C-22)] and seven methyl signals [δ_H 0.96 (3H, s, H-25), 1.01 (3H, s, H-27), 1.03 (3H, s, H-23), 1.04 (3H, s, H-28), 1.07 (3H, s, H-26), 1.08 (3H, s, H-24) and 1.43 (3H, s, H-29); δ_C 15.6 (C-25), 16.6 (C-26), 17.2 (C-28), 18.7 (C-27), 21.1 (C-23), 21.2 (C-29) and 26.6 (C-24)]. Comparison of the ^{1}H- and ^{13}C-NMR data of **1** with those of spergulagenin A (**1a**) [6] suggested that their structures were closely related, except that the carbonyl group [δ_C 217.3 (C-3)] at C-3 of **1** replaced the 3β-hydoxyl group of spergulagenin A (**1a**) [6]. This was supported by both HMBC correlations between H-1, H-2, H-23 and C-3 (δ_C 217.3). The relative stereochemistry of **1** was elucidated on the basis of NOESY experiments (Figure 2). The NOESY cross-peaks between H-5/H-9, H-9/H-12, H-12/H-27, H-13/H-17, H-13/H-26, H-16/H-29, H-23/H-25, H-25/H-26, H-27/H-28, and, H-28/H-29 suggested that H-13, H-17, Me (23), Me (25) and Me (26) on the β-side and H-5, H-9, H-12, H-16, Me (27), Me (28) and Me (29) are on the α-side of **1**. The full assignment of ^{13}C- and ^{1}H-NMR resonances was determined by ^{13}C-DEPT (Figure S4), ^{1}H–^{1}H COSY (Figure S5), NOESY (Figures 3 and S6), HSQC (Figure S7), and HMBC (Figures 3 and S8) techniques. The absolute configuration of **1** was evidenced by the ECD Cotton effects at 284 (Δε +0.88), 250 (Δε −0.12), 217 (Δε +0.98), and 198 (Δε −1.34) nm, in analogy with those of glinusopposide D [11]. According to the evidence above, the structure of **1** was elucidated as (3*R*,4*S*,5aR,5b*R*,11a*R*,13*R*,13b*R*)-3-acetyl-4,13-dihydroxy-3,5a,5b,8,8,11a,13b-heptamethylicosahydro-9*H*-cyclopenta[*a*]chrysen-9-one, named spergulagenin B.

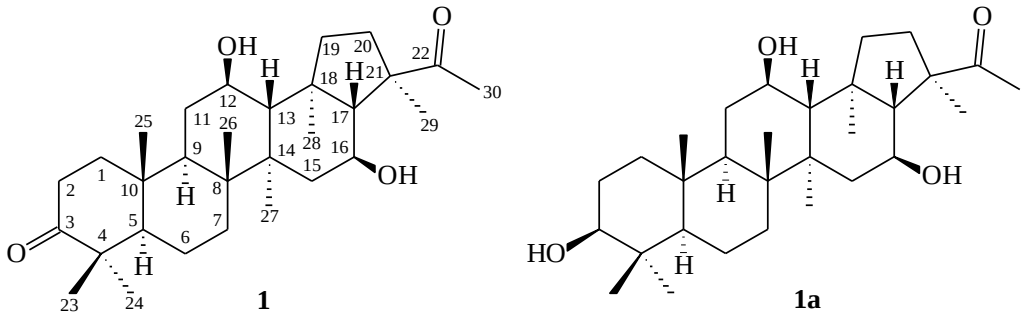

1

1a

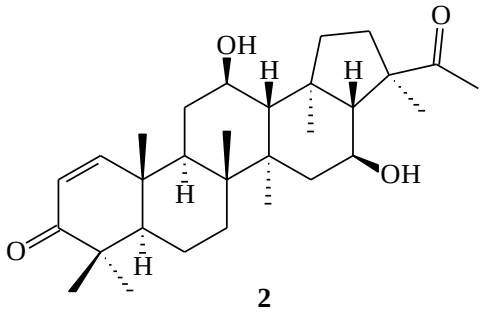

2

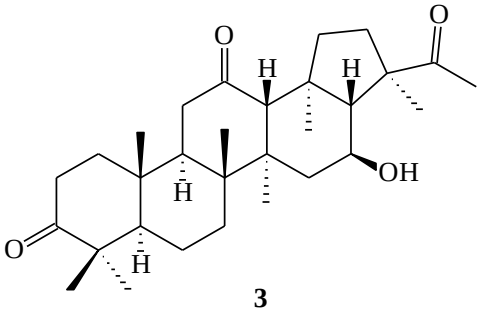

3

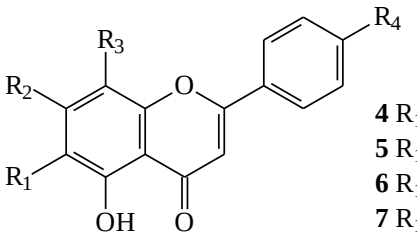

4 $R_1 = R_3 = H$, $R_2 = R_4 = OH$
5 $R_1 = R_3 = Me$, $R_2 = R_4 = OH$
6 $R_1 = R_3 = Me$, $R_2 = OH$, $R_4 = H$
7 $R_1 = R_3 = Me$, $R_2 = OMe$, $R_4 = OH$

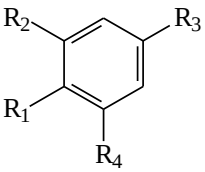

8 $R_1 = OH$, $R_2 = R_4 = H$, $R_3 = COOH$
9 $R_1 = OH$, $R_2 = R_4 = H$, $R_3 = CHO$
10 $R_1 = OH$, $R_2 = R_4 = H$, $R_3 = COMe$
11 $R_1 = OH$, $R_2 = R_4 = H$, $R_3 = COOMe$
12 $R_1 = OMe$, $R_2 = R_4 = H$, $R_3 = COOH$
13 $R_1 = OH$, $R_2 = OMe$, $R_3 = CHO$, $R_4 = H$
14 $R_1 = OH$, $R_2 = OMe$, $R_3 = COMe$, $R_4 = H$
15 $R_1 = OH$, $R_2 = R_4 = OMe$, $R_3 = COMe$
16 $R_1 = OH$, $R_2 = R_4 = OMe$, $R_3 = CHO$
17 $R_1 = OH$, $R_2 = R_4 = H$, $R_3 = CH_2OH$
18 $R_1 = OH$, $R_2 = R_4 = H$, $R_3 = CH_2CH_2OH$
19 $R_1 = OH$, $R_2 = R_4 = H$, $R_3 = HC{=}CHCOOH$
20 $R_1 = OH$, $R_2 = OMe$, $R_3 = HC{=}CHCOOH$, $R_4 = H$

Figure 2. The chemical structures of compounds **1**–**20**.

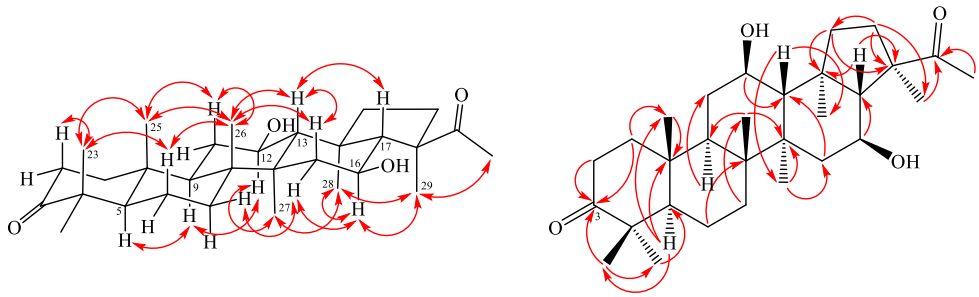

Figure 3. Key NOESY ( ) and HMBC ( ) correlations of **1**.

Spergulagenin C (**2**) was obtained as colorless needle crystal. Its molecular formula, $C_{30}H_{46}O_4$, was confirmed by the positive HR-ESI-MS at *m/z* 470.3409 $[M]^+$ (calculated for $C_{30}H_{46}O_4$, 470.3406) and supported by the ^{13}C, ^1H, and DEPT NMR data. IR absorptions for OH (3493 and 3416 cm^{-1}) functions were observed. The presence of the acetyl group was supported by a band at 1690 cm^{-1} in the IR spectrum and was affirmed by signal at δ 25.9, and δ 217.0 in the ^{13}C-NMR spectrum. The ^{13}C- and ^1H-NMR data of **2** revealed the acetyl group [δ_H 2.24 (3H, s, H-30); δ_C 25.9 (C-30) and 217.0 (C-22)] and seven methyl signals [δ_H 1.01 (3H, s, H-27), 1.04 (3H, s, H-28), 1.08 (3H, s, H-25), 1.09 (3H, s, H-23), 1.11 (3H, s, H-26), 1.14 (3H, s, H-24), and 1.45 (3H, s, H-29); δ_C 17.1 (C-25), 17.2 (C-26), 18.8 (C-28), 18.9 (C-27), 21.4 (C-23), 21.1 (C-29) and 27.8 (C-24)]. The ^1H- and ^{13}C-NMR data of **2** were similar to those of **1**, except that the double bond at C-1,2 [δ_H 5.83, 7.10 (each 1H, each d, *J* = 10.0 Hz, H-2 and H-1); δ_C 125.6 (C-2), 158.5 (C-1)] of **2** replaced C-1,2 single bond [δ_H 1.41, 1.94 (each 1H, m, H-1), 2.42, 2.48 (each 1H, m, H-2); δ_C 34.0 (C-2), 39.4 (C-1)] of **1**. This was supported by the HMBC correlations between H-1 (δ_H 7.10) and C-3 (δ_C 205.3), C-4 (δ_C 39.2), C-5 (δ_C 53.3), and C-9 (δ_C 42.7); and between H-2 (δ_H 5.83) and C-4 (δ_C 39.2) and C-10 (δ_C 44.6). The NOESY cross-peaks between H-5/H-9, H-9/H-12, H-12/H-27, H-13/H-17, H-13/H-26, H-16/H-29, H-23/H-25, H-25/H-26, H-27/H-28, and, H-28/H-29 suggested that H-13, H-17, Me (23), Me (25) and Me (26) are on the β-side and H-5, H-9, H-12, H-16, Me (27), Me (28) and Me (29) are on the α-side of **1**. The full assignment of ^{13}C- and ^1H-NMR resonances was confirmed by ^{13}C-DEPT (Figure S12), ^1H–^1H COSY (Figure S13), NOESY (Figures 4 and S14), HSQC (Figure S15), and HMBC (Figures 4 and S16) techniques. The absolute configuration of **2** was evidenced by the ECD Cotton effects at 283 (Δε +0.96), 249 (Δε −0.14), 219 (Δε +1.05), and 198 (Δε −1.09) nm, in analogy with those of **1** and glinusopposide D [11]. On the basis of the evidence above, the structure of **2** was elucidated as (3*R*,4*S*,5a*R*,5b*R*,11a*R*,13*R*,13b*R*)-3-acetyl-4,13-dihydroxy-3,5a,5b,8,8,11a,13b-heptamethyl-1,2,3,3a,4,5,5a,5b,6,7,7a,8,11a,11b,12,13,13a,13b-octadecahydro-9*H*-cyclopenta[a] chrysen-9-one, named spergulagenin C.

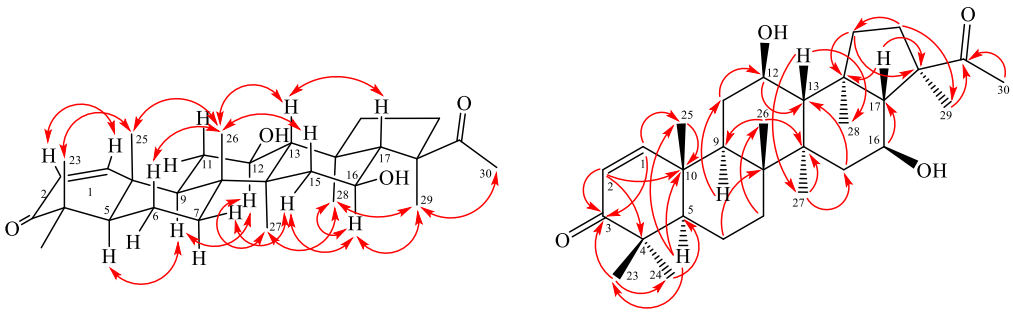

Figure 4. Key NOESY ( ) and HMBC ( ) correlations of **1**.

Spergulagenin D (**3**) was obtained as colorless needle. Its molecular formula, $C_{30}H_{46}O_4$, was determined on the basis of the positive HR-EI-MS at *m/z* 470.3407 $[M]^+$ (calcd. 470.3403) and supported by the ^1H, ^{13}C, and DEPT NMR data. IR absorptions for OH (3447 cm^{-1}) and carbonyl (1697 cm^{-1}) functions were observed. The ^1H- and ^{13}C-NMR data of **3** showed the acetyl group [δ_H 2.24 (3H, s, H-30); δ_C 26.1 (C-30); and 217.3 (C-22)] and seven methyl signals [δ_H 0.99 (3H, s, H-27), 1.00 (3H, s, H-25), 1.06 (3H, s, H-23), 1.10 (3H, s, H-24), 1.14 (3H, s, H-28), 1.21 (3H, s, H-26), and 1.43 (3H, s, H-29); δ_C 15.2 (C-25), 16.7 (C-26), 17.7 (C-28), 20.9 (C-27), 21.4 (C-23), 21.4 (C-29), and 26.6 (C-24)]. The ^1H- and ^{13}C-NMR data of **3** were similar to those of **1**, except that the carbonyl group at C-12 [δ_C 210.9 (C-12)] of **3** replaced the 12β-OH group [δ_H 3.95 (each 1H, m, H-12); δ_C 69.5 (C-12)] of **1**. This was supported by the HMBC correlations between H-11 (δ_H 2.22, 2.25) and C-9 (δ_C 49.6), C-12 (δ_C 210.9); and between H-9 (δ_H 1.70) and C-10 (δ_C 37.0) and C-12 (δ_C 210.9). The relative stereochemistry of **3** was elucidated on the basis of NOESY experiments (Figure 4). The NOESY cross-peaks between H-5/H-9, H-13/H-17,

H-13/H-26, H-16/H-29, H-23/H-25, H-25/H-26, H-27/H-28, and H-28/H-29 suggested that H-13, H-17, Me (23), Me (25) and Me (26) were on the β-side and H-5, H-9, H-16, Me (27), Me (28), and Me (29) were on the α-side of **3**. The full assignment of ^{13}C- and ^{1}H-NMR resonances was determined by ^{13}C-DEPT (Figure S20), ^{1}H–^{1}H COSY (Figure S21), NOESY (Figures 5 and S22), HSQC (Figure S23), and HMBC (Figures 5 and S24) experiments. The absolute configuration of **3** was evidenced by the ECD Cotton effects at 284 (Δε +0.76), 249 (Δε −0.09), 218 (Δε +1.00), and 197 (Δε −0.91) nm, in analogy with those of **1** and glinusopposide D [11]. On the basis of the evidence above, the structure of **3** was elucidated as (3*R*,4*S*,5a*R*,5b*R*,11a*R*,13b*S*)-3-acetyl-4-hydroxy-3,5a,5b,8,8,11a,13b-heptamethyloctadecahydro-9*H*-cyclopenta[*a*]chrysene-9,13(8*H*)-dione, named spergulagenin D.

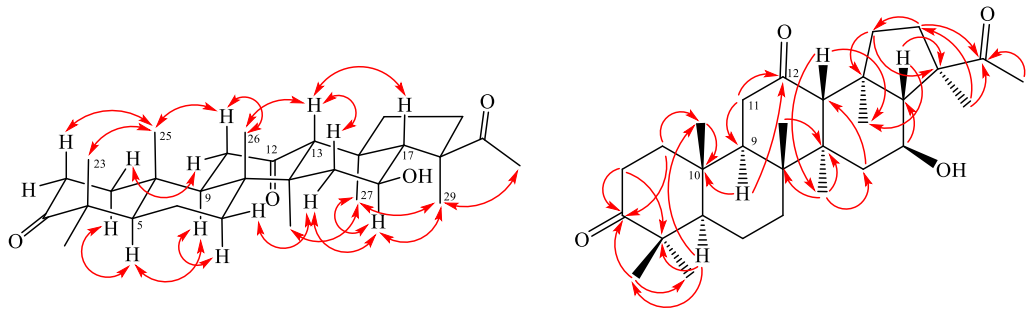

Figure 5. Key NOESY ( ) and HMBC ( ) correlations of **1**.

3.2. Structure Identification of Known Isolated Compounds

The known isolated compounds were readily determined by a comparison of physical and spectroscopic data (^{1}H-NMR, ^{13}C-NMR, MS, UV, and IR) with the literature values or corresponding authentic samples, and this included four flavonoids, kaempferol (**4**) [12], 6, 8-dimethyl-5, 7, 4′-trihydroxyflavone (**5**) [13], 5,7-dihydroxy-6,8-dimethylflavone (**6**) [14], and 5,4′-dihydroxy-7-methoxy-6,8-dimethylflavone (**7**) [15], and thirteen aromatics, 4-hydroxybenzoic acid (**8**) [16], 4-hydroxybenzaldehyde (**9**) [17], 4-hydroxyacetophenone (**10**) [17], methyl 4-Hydroxybenzoate (**11**) [17], *p*-anisic acid (**12**) [18], vanillin (**13**) [19], 4-hydroxy-3-methoxyacetophenone (**14**) [20], acetosyringone (**15**) [21], 4-hydroxy-3,5-dimethoxybenzaldehyde (**16**) [22], 4-hydroxybenzyl alcohol (**17**) [23], 2-(4-hydroxyphenyl) ethanol (**18**) [24], cinnamic acid (**19**) [25], and trans-ferulic acid (**20**) [26].

3.3. Biological Studies

Nitric oxide (NO) is derived from the oxidation of L-arginine by NO synthase (NOS) and is a mediator in the inflammatory response involved in host defense [27]. In inflammation and carcinogenesis conditions, there is an increased production of NO by inducible NO synthase (iNOS) [28]. The anti-inflammatory effects of the compounds isolated from the aerial part of *G. oppositifolius* were also evaluated by suppressing lipopolysaccharide (LPS)-induced NO generation in macrophage cell line RAW264.7. The inhibitory activity data of the isolates **1**–**20** on NO generation by macrophages are shown in Tables 3 and S1. Quercetin was used as the positive control. From the results of our anti-inflammatory tests, the following conclusions can be drawn: (a) Compounds **3**, **5**, **19**, and **20** exhibited inhibitory effects on lipopolysaccharides (LPS)-induced nitric oxide production in RAW 264.7 cells with IC_{50} values of 17.03 ± 1.28, 18.21 ± 1.15, 16.30 ± 1.41, and 12.64 ± 1.14 μM, respectively (Table 1); (b) Among new triterpenoids, spergulagenin D (**3**) (with 3,12-dioxo groups) exhibited more effective inhibition than its analogues, spergulagenin B (**1**) (with 3-oxo-12β-hydroxy groups) and spergulagenin C (**2**) (with 1,2-dehydro-3-oxo-12β-hydroxy groups) against LPS-induced NO generation. (c) Among the flavonoids, 6,8-dimethyl-5,7,4′-trihydroxyflavone (**5**) (with 6,8-dimethyl-5,7,4′-trihydroxy groups) exhibited more effective inhibition than its analogues, kaempferol (**4**) (with 5,7,4′-trihydroxy groups), 5,7-dihydroxy-6,8-dimethylflavone (**6**) (with 5,7-dihydroxy-6,8-dimethyl groups), and

5,4′-dihydroxy-7-methoxy-6,8-dimethylflavone (**7**) (with 5,4′-dihydroxy-7-methoxy-6,8-dimethyl groups) against LPS-induced NO generation. (d) trans-ferulic acid (**20**) is the most effective among the isolated compounds against LPS-induced NO generation. In addition, compounds **3**, **5**, and **20** exhibited inhibitory effects on LPS-induced TNF-α production in RAW 264.7 cells with IC_{50} values of 18.35 ± 1.34, 17.56 ± 1.41, and 14.27 ± 1.29 μM, respectively (Tables 4 and S2).

Table 3. Inhibitory effect of compounds **1**–**20** on production of nitric oxide in LPS-stimulated RAW 264.7 cells.

Compounds	NO Inhibition IC_{50} (μM) [a]
Spergulagenin B (**1**)	24.76 ± 1.41 ***
Spergulagenin C (**2**)	28.26 ± 2.78 **
Spergulagenin D (**3**)	17.03 ± 1.28
Kaempferol (**4**)	38.87 ± 1.68 ***
6,8-Dimethyl-5,7,4′-trihydroxyflavone (**5**)	18.21 ± 1.15
5,7-Dihydroxy-6,8-dimethylflavone (**6**)	43.61 ± 2.96 ***
5,4′-Dihydroxy-7-methoxy-6,8-dimethylflavone (**7**)	32.08 ± 2.75 **
4-Hydroxybenzoic acid (**8**)	75.83 ± 6.63 **
4-Hydroxybenzaldehyde (**9**)	88.20 ± 7.78 **
4-Hydroxyacetophenone (**10**)	76.24 ± 6.55 **
Methyl 4-Hydroxybenzoate (**11**)	78.50 ± 8.00 **
p-Anisic acid (**12**)	115.58 ± 10.35 **
Vanillin (**13**)	94.95 ± 10.99 **
4-Hydroxy-3-methoxyacetophenone (**14**)	111.29 ± 12.91 **
Acetosyringone (**15**)	75.43 ± 6.63 **
4-Hydroxy-3, 5-dimethoxybenzaldehyde (**16**)	86.62 ± 7.74 **
4-Hydroxybenzyl alcohol (**17**)	78.64 ± 7.23 **
2-(4-Hydroxyphenyl)ethanol (**18**)	28.47 ± 1.94 ***
Cinnamic acid (**19**)	16.30 ± 1.41
trans-Ferulic acid (**20**)	12.64 ± 1.14 **
Quercetin [b]	16.74 ± 1.26

[a] The IC_{50} value was defined as half-maximal inhibitory concentration and was expressed as mean ± SD (n = 3); [b] Quercetin was used as positive control; ** $p < 0.01$, and *** $p < 0.001$ compared with the control.

Table 4. Inhibitory effect of compounds **1**–**20** on the production of pro-inflammatory cytokine, TNF-α in LPS-stimulated RAW 264.7 cells.

Compounds	TNF-α Inhibition IC_{50} (μM) [a]
Spergulagenin B (**1**)	30.49 ± 2.20 **
Spergulagenin C (**2**)	31.36 ± 2.59 **
Spergulagenin D (**3**)	18.35 ± 1.34 **
Kaempferol (**4**)	35.71 ± 4.74 *
6,8-Dimethyl-5,7,4′-trihydroxyflavone (**5**)	17.56 ± 1.41 **
5,7-Dihydroxy-6,8-dimethylflavone (**6**)	39.48 ± 3.06 **
5,4′-Dihydroxy-7-methoxy-6,8-dimethylflavone (**7**)	34.17 ± 2.49 **
4-Hydroxybenzoic acid (**8**)	80.02 ± 7.10 **
4-Hydroxybenzaldehyde (**9**)	86.38 ± 6.28 ***
4-Hydroxyacetophenone (**10**)	79.03 ± 5.26 ***
Methyl 4-Hydroxybenzoate (**11**)	82.33 ± 7.25 **
p-Anisic acid (**12**)	125.84 ± 11.47 **
Vanillin (**13**)	102.35 ± 9.36 **
4-Hydroxy-3-methoxyacetophenone (**14**)	123.07 ± 11.37 **
Acetosyringone (**15**)	68.38 ± 5.48 **
4-Hydroxy-3, 5-dimethoxybenzaldehyde (**16**)	77.39 ± 6.73 **
4-Hydroxybenzyl alcohol (**17**)	69.38 ± 6.24 **
2-(4-Hydroxyphenyl)ethanol (**18**)	26.44 ± 2.35 *
Cinnamic acid (**19**)	22.00 ± 1.51 **
trans-Ferulic acid (**20**)	14.27 ± 1.29 **
Quercetin [b]	5.08 ± 0.23

[a] The IC_{50} value was defined as half-maximal inhibitory concentration and was expressed as mean ± SD (n = 3); [b] Quercetin was used as positive control; * $p < 0.05$, ** $p < 0.01$, and *** $p < 0.001$ compared with the control.

The above findings indicated that the promising inhibitory activity against LPS-induced NO and TNF-α generation of *G. oppositifolius* and its isolates could stimulate future development of new anti-inflammatory agents.

4. Conclusions

Twenty compounds, including three new triterpenoids—spergulagenin B (**1**), spergulagenin C (**2**), and spergulagenin D (**3**)—were isolated from aerial part of *G. oppositifolius*. The structures of these new compounds were elucidated on the basis of spectral data. The effects on macrophage pro-inflammatory responses of isolated compounds were evaluated by suppressing LPS-induced NO generation by macrophage RAW264.7 cells. The results of anti-inflammatory assays show that compounds **3**, **5**, **19**, and **20** can obviously inhibit LPS-induced NO generation. Trans-ferulic acid (**20**) is the most effective among the isolated compounds, with IC_{50} value of 12.64 ± 1.14 μM, against LPS-induced NO generation. Furthermore, compounds **3**, **5**, and **20** exhibited inhibitory effects on LPS-induced TNF-α production in RAW 264.7 cells with IC_{50} values of 18.35 ± 1.34, 17.56 ± 1.41, and 14.27 ± 1.29 μM, respectively. Our research indicates *G. oppositifolius* and its isolates (especially **3**, **5**, **19**, and **20**) are worth further research and may be expectantly developed as candidates for the treatment or prevention of various inflammatory diseases (such as dermatitis and arthritis). This study also provides anti-inflammatory scientific evidence for the use of traditional herbal medicine (*G. oppositifolius*) in the treatment of dermatitis and chronic inflammatory diseases [2].

Supplementary Materials: The following supporting information can be downloaded at: https://www.mdpi.com/article/10.3390/molecules28072903/s1, Figure S1: The IR spectrum of **1**; Figure S2: The ^{1}H-NMR spectrum of **1** ($CDCl_3$, 500 MHz); Figure S3: The ^{13}C-NMR spectrum of **1** ($CDCl_3$, 125 MHz); Figure S4: The ^{13}C-DEPT spectrum of **1** ($CDCl_3$, 125 MHz); Figure S5: The ^{1}H–1H COSY spectrum of **1**; Figure S6: The NOESY spectrum of **1**; Figure S7: The HSQC spectrum of **1**; Figure S8: The HMBC spectrum of **1**; Figure S9: The IR spectrum of **2**; Figure S10: The ^{1}H-NMR spectrum of **2** ($CDCl_3$, 500 MHz); Figure S11: The ^{13}C-NMR spectrum of **2** ($CDCl_3$, 125 MHz); Figure S12: The ^{13}C-DEPT spectrum of **2** ($CDCl_3$, 125 MHz); Figure S13: The ^{1}H–^{1}H COSY spectrum of **2**; Figure S14: The NOESY spectrum of **2**; Figure S15: The HSQC spectrum of **2**; Figure S16: The HMBC spectrum of **2**; Figure S17: The IR spectrum of **3**; Figure S18: The ^{1}H-NMR spectrum of **3** ($CDCl_3$, 500 MHz); Figure S19: The ^{13}C-NMR spectrum of **3** ($CDCl_3$, 125 MHz); Figure S20: The ^{13}C-DEPT spectrum of **3** ($CDCl_3$, 125 MHz); Figure S21: The ^{1}H–^{1}H COSY spectrum of **3**; Figure S22: The NOESY spectrum of **3**; Figure S23: The HSQC spectrum of **3**; Figure S24: The HMBC spectrum of **3**; Table S1: Inhibitory effect of compounds **1**–**20** on production of nitric oxide in LPS-stimulated RAW 264.7 cells; Table S2: Inhibitory effect of compounds **1**–**20** on the production of pro-inflammatory, TNF-α in LPS-stimulated RAW 264.7 cells.

Author Contributions: J.-J.C. and C.-S.Y. performed the bioassay, analyzed the data, and wrote the manuscript. Y.-H.C., J.-J.C., C.-Y.C. and Y.-C.C. conducted the isolation and structure elucidation of the constituents. J.-J.C. analyzed bioassay data. J.-J.C. and Y.-H.K. planned, designed, and organized all of the research for this study and prepared the manuscript. All authors have read and agreed to the published version of the manuscript.

Funding: This study was supported by a grant from the Ministry of Science and Technology (MOST), Taiwan (No. MOST 109-2320-B-010-029-MY3), awarded to J.-J. Chen.

Institutional Review Board Statement: Not applicable.

Informed Consent Statement: Not applicable.

Data Availability Statement: The data are contained within the article.

Conflicts of Interest: The authors declare no conflict of interest.

Sample Availability: Samples of the compounds are available from the authors.

References

1. Lu, S.U.; Yang, Y.P. *Molluginaceae in Flora of Taiwan*, 2nd ed.; Editorial Committee of the Flora of Taiwan: Taipei, Taiwan, 1996; pp. 325–328.
2. Sheu, S.Y.; Yao, C.H.; Lei, Y.C.; Kuo, T.F. Recent progress in *Glinus oppositifolius* research. *Phytochem. Pharm. Biol.* **2014**, *52*, 1079–1084. [CrossRef] [PubMed]
3. Yang, C.S.; Huang, H.C.; Wang, S.Y.; Sung, P.J.; Huang, G.J.; Chen, J.J.; Kuo, Y.H. New diphenol and isocoumarins from the aerial part of *Lawsonia inermis* and their inhibitory activities against NO production. *Molecules* **2016**, *21*, 1299. [CrossRef] [PubMed]
4. Ahmed, S.; Rahman, A.; Alam, A.; Saleem, M.; Athar, M.; Sultana, S. Evaluation of the efficacy of *Lawsonia alba* in the alleviation of carbon tetrachloride-induced oxidative stress. *J. Ethnopharmacol.* **2000**, *69*, 157–164. [CrossRef] [PubMed]
5. Liou, J.R.; Mohamed, E.S.; Du, Y.C.; Tseng, C.N.; Hwang, T.L.; Chuang, Y.L.; Hsu, Y.M.; Hsieh, P.W.; Wu, C.C.; Chen, S.L.; et al. 1,5-Diphenylpent-3-en-1-ynes and methyl naphthalene carboxylates from *Lawsonia inermis* and their anti-inflammatory activity. *Phytochemistry* **2013**, *88*, 67–73. [CrossRef]
6. Kitagwa, I.; Yamanaka, H.; Nakanishi, T.; Yosioka, I. Saponin and sapogenol. XXII. Structure of spergulatriol, a new bisnorhopane-type genuine sapogenol of isoanhydrospergulatriol, from the root of *Mollugo spergula* L. *Chem. Pharm. Bull.* **1977**, *25*, 2430–2436. [CrossRef]
7. Karin, M.; Clevers, H. Reparative inflammation takes charge of tissue regeneration. *Nature* **2016**, *529*, 307–315. [CrossRef]
8. Bradley, J.R. TNF-Mediated inflammatory disease. *J. Pathol.* **2008**, *214*, 149–160. [CrossRef]
9. Chen, S.C.; Yang, C.S.; Chen, J.J. Main bioactive components and their biological activities from natural and processed rhizomes of *Polygonum sibiricum*. *Antioxidants* **2022**, *11*, 1383. [CrossRef]
10. Hsu, J.H.; Yang, C.S.; Chen, J.J. Antioxidant, anti-α-glucosidase, antityrosinase, and anti-inflammatory activities of bioactive components from *Morus alba*. *Antioxidants* **2022**, *11*, 2222. [CrossRef]
11. Zhang, D.; Fu, Y.; Yang, J.; Li, X.N.; San, M.M.; Oo, T.N.; Wang, Y.; Yang, X. Triterpenoids and their glycosides from *Glinus oppositifolius* with antifungal activities against *Microsporum gypseum* and *Trichophyton rubrum*. *Molecules* **2019**, *24*, 2206. [CrossRef]
12. Lee, Y.J.; Wu, T.D. Total synthesis of kaempferol and methylated kampferol derivatives. *J. Chin. Chem. Soc.* **2001**, *48*, 201–206. [CrossRef]
13. Youssef, T.A.; Ramadan, M.A.; Khalifa, A.A. Acetophenones, a chalcone, a chromone and flavonoids from *Pancratium maritimum*. *Phytochemistry* **1998**, *8*, 2579–2583. [CrossRef]
14. Kuo, Y.H.; Chu, P.H. Studies on the constituents from the bark of *Bauhinia purpurea*. *J. Chin. Chem. Soc.* **2002**, *49*, 269–274. [CrossRef]
15. Ralf, M. Flavonoids from *Leptrospermum scoparium*. *Phytochemistry* **1990**, *29*, 1340–1342.
16. DellaGreca, M.; Monaco, p.; Pinto, G.; Pollio, A.; Previtera, L.; Temussi, F. Phytotoxicity of low-molecular-weight phenols from olive mill waters. *Bull. Environ. Contam. Toxicol.* **2001**, *67*, 352–359. [CrossRef]
17. Yasuhara, A.; Kasano, A.; Sakamoto, T. An efficient method for the deallylation of allyl aryl ethers using electrochemically generated nickel. *J. Org. Chem.* **1999**, *64*, 4211–4213. [CrossRef]
18. Huang, L.; Nardos, T.; Huang, X. A facile method for oxidation of primary alcohols to carboxylic acids and its application in glycosaminoglycan syntheses. *Chem. Eur. J.* **2006**, *12*, 5246–5252. [CrossRef]
19. Sun, R.; Sacalis, J.N.; Chin, C.K.; Still, C.C. Bioactive aromatic compounds from leaves and stems of *Vanilla fragrans*. *J. Agric. Food. Chem.* **2001**, *49*, 5161–5164. [CrossRef]
20. Syeda, F.A.; Habib-Ur, R.; Atta-Ur, R.M.; Iqbal, C. Phytochemical investigations on *Iris germanica*. *Nat. Prod. Res.* **2010**, *24*, 131–139.
21. Song, Y.N.; Shibuya, M.; Ebizuka, Y.; Sankawa, U. Identification of plant factors inducing virulence gene expression in *Agrobacterium tumefaciens*. *Chem. Pharm. Bull.* **1991**, *39*, 2347–2350. [CrossRef]
22. Lee, T.H.; Chiou, J.L.; Lee, C.K.; Kuo, Y.H. Separation and determination of chemical constituents in the root of *Rhus javanica* L. var. roxburghiana. *J. Chin. Chem. Soc.* **2005**, *52*, 833–841. [CrossRef]
23. Choi, J.H.; Lee, D.U. A new citryl glycoside from *Gastrodia elata* and its inhibitory activity on GABA transaminase. *Chem. Pharm. Bull.* **2006**, *54*, 1720–1721. [CrossRef] [PubMed]
24. Pier, G.B.; Barbara, C.; Romeo, R.; Giampiero, S.; Angela, M.; Ennio, O.; Katia, V.; Pier, A.B. 7-Substituted 5-amino-2-(2-furyl)pyrazolo [4,3-*e*]-1,2,4-triazolo [1,5-*c*]pyrimidines as A_{2a} adenosine receptor antagonists: A study on the importance of modifications at the side chain on the activity and solubility. *J. Med. Chem.* **2002**, *45*, 115–126.
25. Miyazawa, M.; Okuno, Y.; Nakamura, S.; Kameoka, H. Suppression of SOS inducing activity of chemical mutagens by cinnamic acid derivatives from *Scrophulia nangpoensis* in the *Salmonella typhimurium* TA1536/pSK-1002 umu test. *J. Agric. Food Chem.* **1998**, *46*, 904–910. [CrossRef]
26. Supaluk, P.; Saowapa, S.; Apilak, W.; Ratana, L.; Somsak, R.; Virapong, P. Bioactive metabolites from *Spilanthes acmella* Murr. *Molecules* **2009**, *14*, 850–867.
27. Geller, D.A.; Billiar, T.R. Molecular biology of nitric oxide synthases. *Cancer Metastasis Rev.* **1998**, *17*, 7–23. [CrossRef]
28. Moncada, S.; Palmer, R.M.; Higgs, E.A. Nitric oxide: Physiology, pathophysiology, and pharmacology. *Pharmcol. Rev.* **1991**, *43*, 109–142.